



Biomaterials-based Immunomodulation Enhances Survival of Murine Vascularized Composite Allografts

Journal:	<i>Biomaterials Science</i>
Manuscript ID	BM-ART-11-2022-001845.R1
Article Type:	Paper
Date Submitted by the Author:	23-Feb-2023
Complete List of Authors:	<p>Sommerfeld, Sven; Johns Hopkins University School of Medicine, Translational Tissue Engineering Center, Department of Ophthalmology Zhou, Xianyu; Johns Hopkins Medicine School of Medicine, Department of Plastic and Reconstructive Surgery, Vascularized Composite Allotransplantation Laboratory; Shanghai Jiao Tong University School of Medicine, Department of Plastic and Reconstructive Surgery, the Ninth People's Hospital</p> <p>Mejías, Joscelyn; Johns Hopkins University School of Medicine, Translational Tissue Engineering Center, Department of Ophthalmology Oh, Byoung; Johns Hopkins School of Medicine, Department of Plastic and Reconstructive Surgery, Vascularized Composite Allotransplantation Laboratory</p> <p>Maestas, Jr., David; Johns Hopkins University School of Medicine, Translational Tissue Engineering Center, Department of Ophthalmology ; Johns Hopkins School of Medicine, Department of Biomedical Engineering and the Bloomberg-Kimmel Institute for Cancer Immunotherapy</p> <p>Laffont, Philippe; Johns Hopkins Medicine School of Medicine, Translational Tissue Engineering Center, Department of Ophthalmology Furtmüller, Georg; Johns Hopkins Medicine School of Medicine, Department of Plastic and Reconstructive Surgery, Vascularized Composite Allotransplantation Laboratory</p> <p>Elisseeff, Jennifer; Johns Hopkins Medicine School of Medicine, Translational Tissue Engineering Center, Department of Ophthalmology ; Johns Hopkins Medicine School of Medicine, Department of Biomedical Engineering and the Bloomberg-Kimmel Institution for Cancer Immunotherapy</p> <p>Brandacher, Gerald; Johns Hopkins Medicine School of Medicine, Department of Plastic and Reconstructive Surgery, Vascularized Composite Allotransplantation Laboratory</p>

Biomaterials-based Immunomodulation Enhances Survival of Murine Vascularized Composite Allografts

Sven D. Sommerfeld, PhD¹, Xianyu Zhou, MD, PhD^{2,3}, Joscelyn C. Mejías¹, PhD, Byoung Chol Oh, DVM, PhD², David R. Maestas, Jr. PhD^{1,4}, Georg J. Furtmüller, MD², Philippe A. Laffont¹, Jennifer H. Elisseeff, PhD^{1,4**}, Gerald Brandacher, MD^{2**}

¹Translational Tissue Engineering Center, Department of Ophthalmology, Johns Hopkins University School of Medicine, Baltimore, MD

²Department of Plastic and Reconstructive Surgery, Vascularized Composite Allotransplantation (VCA) Laboratory, Johns Hopkins School of Medicine, Baltimore, MD

³Department of Plastic and Reconstructive Surgery, the Ninth People's Hospital, Shanghai Jiao Tong University School of Medicine, Shanghai, People's Republic of China.

⁴Department of Biomedical Engineering and the Bloomberg-Kimmel Institute for Cancer Immunotherapy, Johns Hopkins University School of Medicine, Baltimore, MD

**To whom correspondence should be addressed: Jennifer Elisseeff, jhe@jhu.edu, and Gerald Brandacher, brandacher@jhmi.edu

Authorship note: SDS, XZ, JCM are co-first and JHE and GB co-corresponding

Abstract

Vascularized composite allotransplantation (VCA) is a restorative option for patients suffering from severe tissue defects not amenable to conventional reconstruction. However, the toxicities associated with life-long multidrug immunosuppression to enable allograft survival and induce immune tolerance largely limits the broader application of VCA. Here, we investigate the potential of targeted immunomodulation using CTLA4-Ig combined with a biological porcine-derived extracellular matrix (ECM) scaffold that elicits a pro-regenerative Th2 response to promote allograft survival and regulate the inflammatory microenvironment in a stringent mouse orthotopic hind limb transplantation model (BALB/c to C57BL/6). The median allograft survival time (MST) increased significantly from 15.0 to 24.5 days ($P = 0.0037$; Mantel-Cox test) after adding ECM to the CTLA4-Ig regimen. Characterization of the immune infiltration shows a pro-regenerative phenotype prevails over those associated with inflammation and rejection including macrophages (F4/80^{hi}CD206^{hi}MHCII^{low}), eosinophils (F4/80^{low}Siglec-F⁺), and T helper 2 (Th2) T cells (CD4⁺IL-4⁺). This was accompanied by an increased expression of genes associated with a Type 2 polarized immune state such as *Il4*, *Ccl24*, *Arg1* and *Ym1* within the graft. Furthermore, when ECM was applied along with a clinically relevant combination of CTLA4-Ig and Rapamycin, allograft survival was prolonged from 33.0 to 72.5 days ($P = 0.0067$; Mantel-Cox test). These studies implicate the clinical exploration of combined regimens involving local application of pro-regenerative, immunomodulatory biomaterials in surgical wound sites with targeted co-stimulatory blockade to reduce adverse effects of immunosuppression and enhance graft survival in VCA.

Introduction

Vascularized composite allotransplantation (VCA) is a promising reconstructive strategy for patients suffering from devastating tissue loss requiring major reconstruction such as hand and face transplantation. VCA is unique in that combinations of muscle, bone, nerve, and skin are transplanted as a unit allowing for “like-with-like” replacement and functional restoration^{1, 2}. An important element for the clinical advancement of VCAs is to develop regimens that prevent rejection by targeting known immune mechanisms known to influence the success of the transplant. The tissue damage and inflammation inevitably caused by ischemia inherent to the surgery combined with the toxicity and adverse effects from high dosages of multiple immunosuppressant drugs to prevent rejection remains a major clinical limitation^{3, 4}. Immunosuppressive agents are implicated in the pathogenesis of organ failure and accelerated cardiovascular disease; the latter of which is a leading cause of death in transplant recipients^{5, 6}. A regimen that reduces the reliance on long-term, high dose immunosuppression would alter the risk-benefit equation for reconstructive transplantation and pave the way for its widespread application.

Ischemia-reperfusion injury (IRI) is an unavoidable series of events that initiates a potent pro-inflammatory response that is proportional to posttransplant graft dysfunction and rejection⁷⁻⁹. Ischemia causes a hypoxia-driven cellular dysfunction that manifests as cell apoptosis or necrosis combined with reperfusion which releases reactive oxygen species further damaging tissues. The increase in damage associated molecular patterns results in upregulation of complement, inflammatory cytokines, as well as activation and migration of leukocytes into the graft. IRI, characterized in murine skin grafts, creates a pro-inflammatory cytokine milieu (TNF- α , IFN- γ , IL-1 β), with increased expression of Major Histocompatibility Complex (MHC) II, and leads to enhanced alloreactivity¹⁰. The injury pattern and surgical trauma creates a pro-inflammatory microenvironment within the VCA that primes the VCA immune response towards rejection^{11, 12}. While there have been advances in methods to minimize ischemia including pre-conditioning, hypothermia, and preservation solutions, the potential benefits of targeting the surgical wounds with Type 2 immune skewing biomaterial to reduce the alloimmune response has not yet been well investigated.

Alloreactivity is the most significant threat leading to acute rejection by the direct recognition of MHC mismatched donor cells by recipient T cells¹³. Costimulatory blockades such as CTLA4-Ig have been developed to specifically block the T cell costimulation instrumental in the immune response leading to graft rejection. Multiple groups have demonstrated efficacy of CTLA4-Ig combination therapies to promote tolerance *in vivo* using rodent models of

allograft transplantation¹⁴⁻¹⁷. Clinically CTLA4-Ig has been used to lower the dose of calcineurin inhibitors to reduce toxicity^{18, 19}. Additionally, the pro-inflammatory environment has been suggested as a primary factor in the disappointing efficacy of CTLA4-Ig^{10, 18}. Development of novel immunomodulatory strategies to reduce the high dose immunosuppression therapeutics is of high importance and necessity. Modulating the immune infiltration into the graft through local delivery of a biomaterial may promote the efficacy of costimulatory blockade.

Biologic scaffolds derived from tissue extracellular matrix (ECM) are used clinically for tissue repair in a variety of scenarios including abdominal wall repair, diabetic ulcer treatment, skin wound repair, and treatment of other soft tissue defects²⁰⁻²⁵. As ECM scaffolds are derived from native tissues, the decellularized scaffold is a complex structural and biochemical mixture that can vary broadly depending on the tissue source (allogeneic or xenogeneic), organ, and decellularization process. While different ECM scaffolds derived from various tissue sources can have differential immune responses (fibrotic vs regenerative), there are many types of ECM scaffolds that can promote an early M2-like macrophage phenotype which correlates to a pro-healing wound environment in severe muscle injuries²⁶⁻²⁸. Here we use a commercially available decellularized urinary bladder matrix particulate (MatriStem, ACell) which has been used clinically^{29,30} and has been shown to promote an M2-like response in injury models such as skeletal muscle and cancer³¹⁻³³. Studies demonstrated that pro-regenerative ECM materials modulate macrophage expression of CD86 and CD206 towards an M2-biased macrophage phenotype and promotes Th2 cells that positively correlated with tissue repair³⁴⁻³⁶. More specifically, the CD4⁺ Th2 T cell adaptive immune response modulates local myeloid cells towards pro-regenerative phenotypes in an IL-4 dependent manner³⁷. Type 2 immunity, including Th2 T cells and M2 macrophages, is associated with regeneration and healing^{38,39} in multiple tissues including skin⁴⁰, muscle⁴¹, and bone^{42,43}. In this work we demonstrate the efficacy of incorporating local delivery of decellularized urinary bladder extracellular matrix in combination with systemic delivery of costimulatory blockade in a murine orthotopic hindlimb transplant model to attenuate and alter the local immune-wound microenvironment. We hypothesize that the local delivery of ECM synergizes with the systemic costimulatory blockade to mitigate the rejection of the donor tissue.

Results

Combination regimen of locally delivered ECM with systemic CTLA4-Ig prolongs VCA graft survival.

ECM when delivered locally to muscle injury modulates the local microenvironment promoting repair through pro-regenerative macrophage polarization and increased recruitment of IL-4 producing cells^{26, 34}. To test the effects of ECM implantation on VCA survival, we used a fully MHC-mismatched murine orthotopic hind limb transplant model (BALB/c [H-2^d] to C57BL6/J [H-2^b]); this model results in clinical rejection of the graft with increased immune infiltration from the host attacking and damaging the donor limb⁴⁴. To test the local implantation of ECM to modulate the immune infiltration into the VCA the following groups were tested: untreated VCA with no therapeutic intervention (Untreated), VCA with ECM added to the interface of the wound just before skin closure (ECM), VCA with CTLA4-Ig delivered IP on days 0, 2, 4, 6 (CTLA4-Ig), VCA with ECM added to the wound and CTLA4-Ig delivered IP on days 0, 2, 4, 6 (CTLA4-Ig + ECM), Figure 1A. The ECM is a commercially available powder (MatriStem) that was resuspended in saline to form a paste for application and was not further processed or crosslinked during application. The combination of ECM with systemic CTLA4-Ig significantly increased graft survival to 24.5 days compared to 9 days for untreated or treated with ECM alone, while systemic CTLA4-Ig without ECM only increased graft survival to 15 days. ($P < 0.0001$; Mantel-Cox) Figure 1B. Histological assessment with Masson's trichrome staining revealed immune cell infiltration in both groups, however, the systemic CTLA4-Ig with ECM treatment maintained immune cell infiltration localized to specific regions while the CTLA4-Ig only group showed a much higher presence of cell infiltration distributed heavily throughout the intragraft muscle component, Figure 1C.

ECM with co-stimulatory blockade reshapes myeloid immune infiltration phenotypes.

Monocytes and macrophages are known to mediate inflammatory and repair processes. Flow cytometry was used to evaluate the effects of ECM with CTLA4-Ig, macrophages (CD64⁺F4/80^{hi}), eosinophils (Siglec-F⁺F4/80^{low}CD64⁻), granulocytes (Ly6c^{mid}), and monocytes (Ly6C^{hi}) at the graft interface on postoperative day (POD) 14, Figure 2A. There were minimal increases in eosinophils, monocytes, and granulocytes between treatment with and without ECM, however, there was significant increase in the number of macrophages ($2.3 \pm 0.2e6$ [Mean \pm SEM] to $4.2 \pm 0.5e6$ cells/g), Figure 2B. To determine macrophage polarization, CD206 (pro-regenerative), CD86 (pro-fibrotic), and MHCII (antigen presentation) mean fluorescence intensity (MFI) was normalized for each surface marker to the systemic CTLA4-Ig expression. While the CD86 and MHCII were not significantly different between treatments, CD206 was 1.7-fold higher

with ECM treatment. Macrophage subsets (CD64⁺F4/80^{hi}) and phenotypic shifts were visualized using the dimensionality reduction algorithm tSNE, Figure 2D. The CTLA4-Ig treatment is enriched for CD86⁺MHCII^{hi} macrophages while the addition of ECM shifts the macrophages to a CD206^{hi}MHCII^{low} phenotype. Immunofluorescent staining of the myeloid marker F4/80 reveals myeloid distribution across the surgical site and infiltration into the ECM, Figure 2E. These results show the addition of ECM not only increases the myeloid fraction of immune cell infiltrates but promotes a more pro-regenerative Type 2 phenotype within these myeloid subsets.

ECM with costimulatory blockade promote a pro-regenerative T helper 2 response in CD4 T cells.

Hind limb grafts from C57BL6/J donors were transplanted onto 4Get IL-4 mouse line recipients to measure changes in CD4 IL-4 by GFP expression via flow cytometry, Figure 3A. Treatment with CTLA4-Ig and ECM decreased the percentage of CD8 T cells in the CD45 population (11% to 7.2%) and increased the percentage of CD4 T cells in the allograft (3.7% to 6.7%), Figure 3B. Within the CD4 T cell population IL-4 expression increased significantly from 6.1% to 25.7%, Figure 3C. Using C57BL6/J recipient mice with stimulation and intracellular staining, Figure 3D, similar trends were observed with IL-4 increasing from 0.3% to 6%, Figure 3E-F. No changes were seen in T helper 1 (Th1) IFN- γ by flow, supplemental figure 1. Gene expression of the proximal tissue isolate showed significant changes in increases in Type 2 related genes and no significant changes in Type 1 related genes.

Short-course Rapamycin further extends transplant survival.

The mTOR inhibitor rapamycin has been reported to be synergistic with CTLA4-Ig blockade in promoting long-term murine allograft survival by attenuating the development of chronic allograft vasculopathy and decreasing the level of fibrosis observed with suboptimal costimulatory blockade therapy alone^{15, 16, 45-48}. To assess if ECM was synergistic with rapamycin and costimulatory blockade, VCA mice were treated with CTLA4-Ig delivered IP on days 0, 2, 4, 6 and an additional 10-day short-course of rapamycin delivered IP on days 0-9 (CTLA4-IG + Rapa) and with ECM implanted at the surgical site (CTLA4-IG + Rapa + ECM). Control VCA mice without ECM had an MST of 34 days and mice treated with ECM had a significant increase in survival of 70 days ($P = 0.0051$; Mantel-Cox), Figure 4A.

Discussion

In reconstructive transplantation, the ultimate goal is to achieve immune tolerance to allow withdrawal of immunosuppressants and avoidance of their long-term adverse effects. Although

immune tolerance has been achieved for a few types of solid organ transplantation (SOT) in clinic⁴⁹⁻⁵¹ and several rodent animal VCA models^{15, 52}, it has not been established in clinical VCA practice. Therefore, there remains a substantial and unmet need to develop novel strategies to increase the efficacy and reduce the toxicity of current treatment regimens for VCA. In this present study we demonstrated the use of a pro-regenerative immunotherapy to prolong VCA graft survival by means of porcine-derived ECM at the surgical interface and systemic delivery of CTLA4-Ig, which facilitated attenuation of immune rejection and prolonged graft survival.

VCA has become a viable surgical technique for “like-with-like” reconstruction of devastating composite tissue loss not amenable to conventional approaches^{4, 53}. However, side effects and toxicities resulting from long-term administration of immunosuppressants, such as infection, tumorigenesis, nephrotoxicity, hepatotoxicity, vasculopathy, are major hurdles for broader implementation. Local immunomodulation specifically tailored to VCA instead of systemic drug delivery may tilt the risk benefit ratio. Biologic scaffolds such as ECM are a promising immunomodulatory tool that provides a complex mixture of biochemical and biomechanical cues to the cells within the tissue-injury microenvironment. These biodegradable scaffolds are fabricated from decellularized heterologous tissues and are available as clinical products. ECM derived from porcine small intestine, porcine urinary bladder, and human dermis have gained clinical acceptance for use in wound healing and reconstructive surgery applications, and several other ECM sources, such as autologous adipose tissue ECM, are currently in clinical trials^{20, 29, 54}.

ECM is a bioactive material that promotes tissue regeneration through angiogenesis, immune and progenitor cell recruitment, and altering the immune response phenotype through Type 2 immune skewing in several murine wound injury models such as cornea⁵⁵, cardiac⁵⁶, abdominal injuries⁵⁷, and skeletal muscle^{34, 58}. Volumetric muscle loss *in vivo* mouse studies using ECM have shown constructive remodeling of innervated and vascularized skeletal muscle as well as rapid and robust macrophage transition from an injury induced pro-inflammatory phenotype to a pro-regenerative phenotype^{27, 34, 58, 59}. The exact mechanism by which ECM promotes regeneration is still largely unknown, however ECM is diverse composition of collagens, proteoglycans, growth factors, cytokines, cellular debris, and extracellular vesicles that give instructive signals to the local microenvironment that are capable of modulating the local immune response^{28, 32, 60}. Choosing a commercially available product provides clinical relevance and consistency of the product that is FDA approved. ECMs derived from different tissues other than porcine urinary bladder matrix have varying compositions that may produce some differential effects however our previous data suggests it is the local environment that is most critical in

determining the immune response²⁸. Additionally, any changes in mechanical properties or the degradation rate of the biomaterial that arise from using a different material source as well as decellularization process may impact the immune response. A prolonged degradation rate can promote fibrosis, and changing the material stiffness, elasticity, or surface topography can all alter macrophage and T cell polarization^{61, 62}.

Macrophage polarization extremes are canonically described as M1, classically activated, or M2, alternatively activated. M1 related pro-inflammatory cytokines such as IL-1 β , TNF- α , IFN- γ are abundantly expressed in damage tissues such as muscle injury. VCAs create extensive surgical damage and these inflammatory cytokine expression patterns are similar to wound inflammation. Macrophage polarization and transition between a pro-inflammatory M1-like to pro-regenerative M2-like phenotypes is critical to the wound healing process. The surgical requirements for a VCA are known to create a highly pro-inflammatory microenvironment, this has opened opportunities for biomaterials to target this pro-inflammatory phenotype and redirect the immune system towards a pro-regenerative M2-like state. Polarization of initial macrophage response to injury is inherently linked to T cell response and phenotype. Using a biomaterial at the interface to promote a more pro-regenerative response in the immune infiltrate of the graft synergizes with the systemic costimulatory blockade to promote the graft survival.

While T cell subsets play pivotal roles in rejection, the outcomes associated with Th1, Th2 and Th17 appears to be context dependent. The full activation of naive T-cells requires the integration of several signals; in addition to the primary antigen-specific signal, the engagement of co-stimulatory receptors such as CD28/CTLA4 are required. The natural ligands to these receptors, CD80/CD86, are found on antigen-presenting cells such as dendritic cells, macrophages, monocytes. CTLA4-Ig, a costimulatory blockage was used here as it has previously been shown to efficiently block CD28/CTLA-4 interaction with their CD80/CD86 ligands to prolong graft acceptance. CTLA4-Ig based immunomodulatory treatment protocols allow reduced overall toxicity of high intensity induction regimens⁶³ and facilitate vascularized osteomyocutaneous allograft survival in rodents, displaying promising potential in VCA⁶⁴.

In this study, we have used a full MHC mismatched VCA murine orthotopic hind limb model which results in acute rejection without intervention. We investigated how local application of ECM at the wound interface of murine VCA injuries shifted immune cell phenotypes in this severe wound microenvironment. We have shown that although implantation of ECM alone in murine VCA does not delay graft rejection, when treated in combination with CTLA4-Ig and rapamycin, graft median survival time can be significantly increased. Rapamycin is an mTOR inhibitor that broadly modulates alloreactivity⁶⁵ and has been clinically shown to synergize with CTLA4-Ig in

renal transplantation⁶⁶. The combination therapy showed shifts in both the myeloid and lymphoid populations into a more pro-regenerative Type 2 phenotype with increased CD206⁺ macrophages and a dominant IL-4⁺ CD4⁺ T cells. It is possible that the effect of ECM downregulating CD80/CD86 in the infiltration of antigen presenting cells with the CTLA4-Ig blockade promotes this Type 2 response to prolong graft survival. This study demonstrates that ECM combined with short-term immunosuppressants prolongs allograft survival in a Type 2 dependent manner at the surgical site. The current clinical availability of these materials makes the translation of the technology concept feasible and show potential for future clinical applications in VCA.

Materials and Methods

Surgical Procedure and Implantation

All animals were housed in a pathogen-free facility and all procedures were performed in compliance with ethical guidelines and protocols approved by the Johns Hopkins University Animal Care and Use Committee (ACUC) and following AAALAC guidelines (protocol no. M16M372). Male 6- to 8-week-old wild type BALB/c or C57BL6/J were purchased from The Jackson Laboratory and C.129-II4^{tm1Lky}/J (IL4-GFP, 4Get) breeding pair were purchased from The Jackson Laboratory.

Orthotopic Hind Limb Allograft Transplantation

BALB/c (donor) hind limb was orthotopically transplanted to C57BL/6 (recipient) or C57BL6/J (donor) were transplanted to 4Get mice using a “Cuff” technique described by Furtmüller et al. (12). Daily visual inspection was performed to monitor graft survival. The endpoint in this study was defined as Grade III allograft rejection (skin epidermolysis) based on Banff classification, 2007⁶⁷. Recipients received analgesia with Buprenorphine at a dose of 0.1 mg/kg subcutaneously every 6-8 hours for 3 days.

Treatment Protocols

30 mg of biologic scaffold material composed of decellularized urinary bladder matrix (Matristem, Acell) was resuspended in phosphate-buffered saline (PBS) at 400 mg/ml then injected into the interface and the subcutaneous space surrounding the approximation site of the donor and recipient musculature followed by skin closure, supplemental figure 2. CTLA4-Ig (Abatacept; Bristol-Myers), was administered on days 0, 2, 4, 6 (500 µg/dose i.p.). Systemic Rapamycin (LC Laboratories) was administered on days 0-9 (1 mg/kg, i.p.) for a 10-day short-course dosage. Mice were euthanized and tissues harvested on POD 14 or when protocol terminal endpoint criteria were met.

Tissue digestion

The donor and recipient quadriceps femoris and biceps femoris interface were finely diced and digested for 45 min at 37°C with 1.67 Wunsch U/ml Liberase TL (Roche Diagnostics) and 0.2 mg/ml DNase I (Roche Diagnostics) in RPMI 1640 medium (Gibco). Digested tissue was then ground through 70 µm strainers (ThermoFisher Scientific) and rinsed with 1X DPBS + 0.05% bovine serum albumin then washed twice with 1X DPBS. This single cell suspension was directly

used for myeloid characterization and lymphocytes were further isolated using a Percoll gradient.

Flow Cytometry Staining (stim)

For flow cytometry surface staining, single cell suspensions were stained for 20 minutes at 4°C using Viability Dye eFluor™ 780 (eBioscience) then stained for 30 minutes at 4°C with a surface antibody cocktail including anti-CD16/32 in a 1% BSA PBS buffer. Myeloid cells were characterized as previously described⁵⁴. Antibodies used can be found in Supplemental Table 1. For intracellular staining, cells were first stimulated at 37°C for 4 hours with the Cell Stimulation Cocktail with protein transport inhibitors (eBioscience) diluted in RPMI supplemented with 5% FBS and 1% penicillin/streptomycin. Cells were then surface stained and fixed/permeabilized with Cytofix/Cytoperm (BD Bioscience) before intracellular staining for 30 minutes at 4°C. Data were collected on an Attune NxT Flow Cytometer (ThermoFisher Scientific) or an LSR II (BD Bioscience) flow cytometer and analyzed using FlowJo software (Treestar), tSNE projections were made with the FlowJo plugin.

qRT-PCR

Total and enriched mRNA was isolated from whole tissue using TRIzol reagent and Qiagen's RNeasy PLUS kits, and was stored in RNase-free Tris-EDTA buffer (pH 7.0) at -80°C. All samples were confirmed to have a 260/280 ratio greater than 1.8, assessed by UV/vis (NanoDrop2000, ThermoFisher Scientific). All qRT-PCR was performed using TaqMan Gene Expression Master Mix (Applied Biosystems) according to manufacturer's instructions and recommendations, TaqMan Assay Probes are listed in Supplemental Table 2. Briefly, 2.5 µg of enriched mRNA was used to synthesize cDNA using Superscript IV VILO Master Mix (ThermoFisher Scientific). The cDNA concentration was set to 100 ng/well (in a total volume of 20 µL PCR reaction). The qRT-PCR reactions were performed on the StepOne Plus Real-Time PCR System (ThermoFisher Scientific), as TaqMan single-plex assays, TaqMan Gene Expression Master Mix was used, and reaction cycles were performed using manufacturer recommended settings for quantitative relative expression. For all muscle tissue samples, *B2m* and *Rer1* were used as the reference gene and test samples were normalized to treated biological controls. All qRT-PCR data was analyzed using the Livak Method, wherein $\Delta\Delta Ct$ values are calculated and reported as relative quantification values (RQ) calculated by $2^{-\Delta\Delta Ct}$ ⁶⁸. Gene expression data from qRT-PCR assays are displayed as $\text{Log}_2(\text{Fold Change})$, same as $\text{Log}_2(\text{RQ})$, with bar plots representing the mean \pm SD.

Histology

Tissue was fixed in 10 % neutral buffered formalin for 48 hours before a graded ethanol and dehydration and cleared for 2.25 hours in xylenes. Briefly, samples were treated in a graded 70 %, 80 %, 95 % (2x), 100 % (3x) ethanol series for 1 hour each then 3x with xylene for 45 minutes each before paraffin infiltration and embedding. 7 μ m thick sections taken using a microtome (Leica RM2255), Muscle sections were stained with Masson's trichrome (Sigma, USA) to visualize cell morphology and collagen deposition. Brightfield imaging was performed using a Zeiss Axio Imager A2 microscope.

Statistical Analysis

Data were analyzed using Graphpad Prism 9.3.1 (Graphpad Software Inc, CA). Statistical significance was determined using student's t-test or two-way ANOVA with Šidák's multiple comparison test. Median survival and Kaplan-Meier survival curves were generated, and Mantel Cox tests were performed for significance. Statistical analyses of qRT-PCR gene expression results were performed on $\text{Log}_2(\text{FC})$ values, using two-way ANOVA with multiple comparisons (each gene compared between test and control separately) using Šidák correction. Gene expression significant differences were further compared with False Discovery-Rate results from multiple t-tests (two-stage step-up method of Benjamini, Keiger, & Yekutieli). P values less than 0.05 were considered statistically significant and denoted by * $p < 0.05$, ** $p < 0.01$, *** $p < 0.001$, and **** $p < 0.0001$.

Acknowledgements

This work was funded in part by the NIH Director's Pioneer Award (J.H.E. #5DP1AR076959), Johns Hopkins Medicine Synergy and Innovation Award (J.H.E. and G.B.), the Morton Goldberg Professorship, and the National Science Foundation Graduate Research Fellowship Program (D.M. #DGE-1746891). The table of contents image was created with BioRender.com.

Competing interests: J.H.E holds equity in Unity Biotechnology, Aegeria Soft Tissue. All other authors declare that they have no competing interests in this study. J.H.E. was previously a member of the scientific advisory board for ACell Inc. (now owned by Integra)

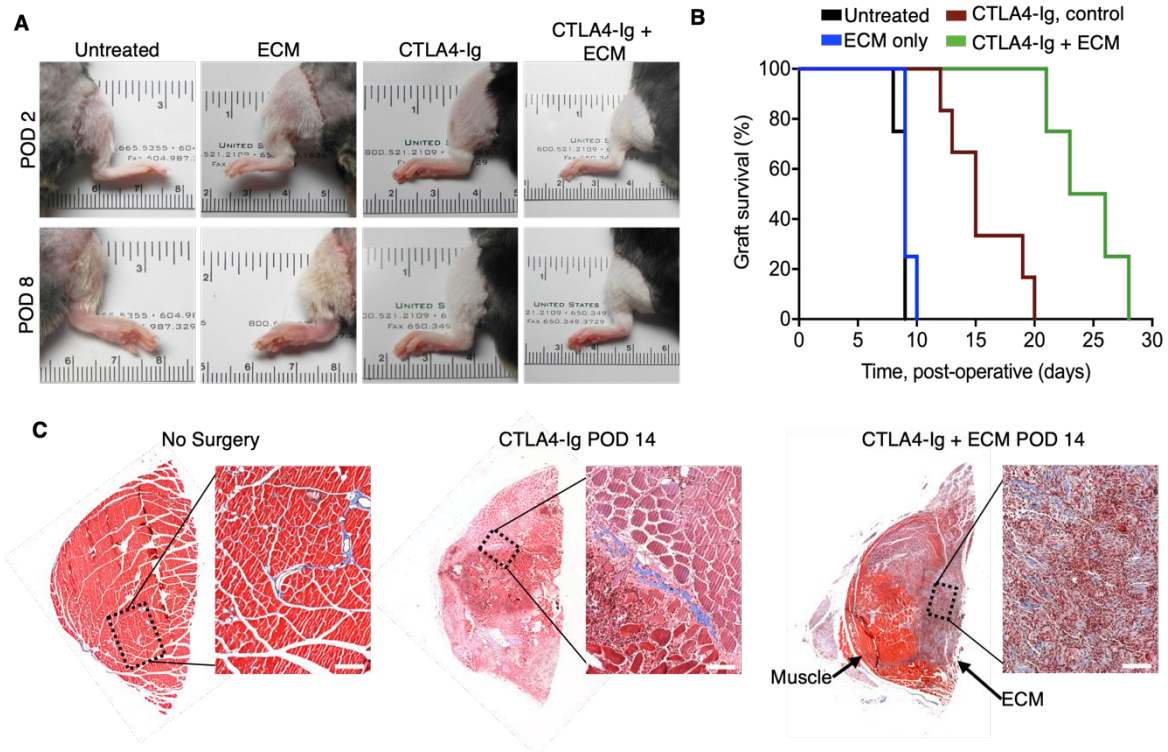


Figure 1: Application of biological scaffolds with co-stimulatory blockade prolongs graft survival. (A) Representative image of the VCA murine orthotopic hindlimb allogeneic transplant model (BALB/c onto C57BL6/J). (B) Graft survival was prolonged with combination CTLA4-Ig and ECM treatment (MST = 24.5, $n = 4$, $P < 0.0001$; Mantel-Cox), with CTLA4-Ig ($n=6$) MST at 15 days and untreated ($n=4$) VCA and ECM ($n=4$) treated VCA MST at 9 days. (C) Representative Masson's trichrome staining of unoperated control and transplanted muscle treated with systemic CTLA4-Ig with or without ECM implantation. The muscle and location of the ECM are labeled in the CTLA4-Ig + ECM POD 14 sample. Inset image scale bar (white) = 100 μ m.

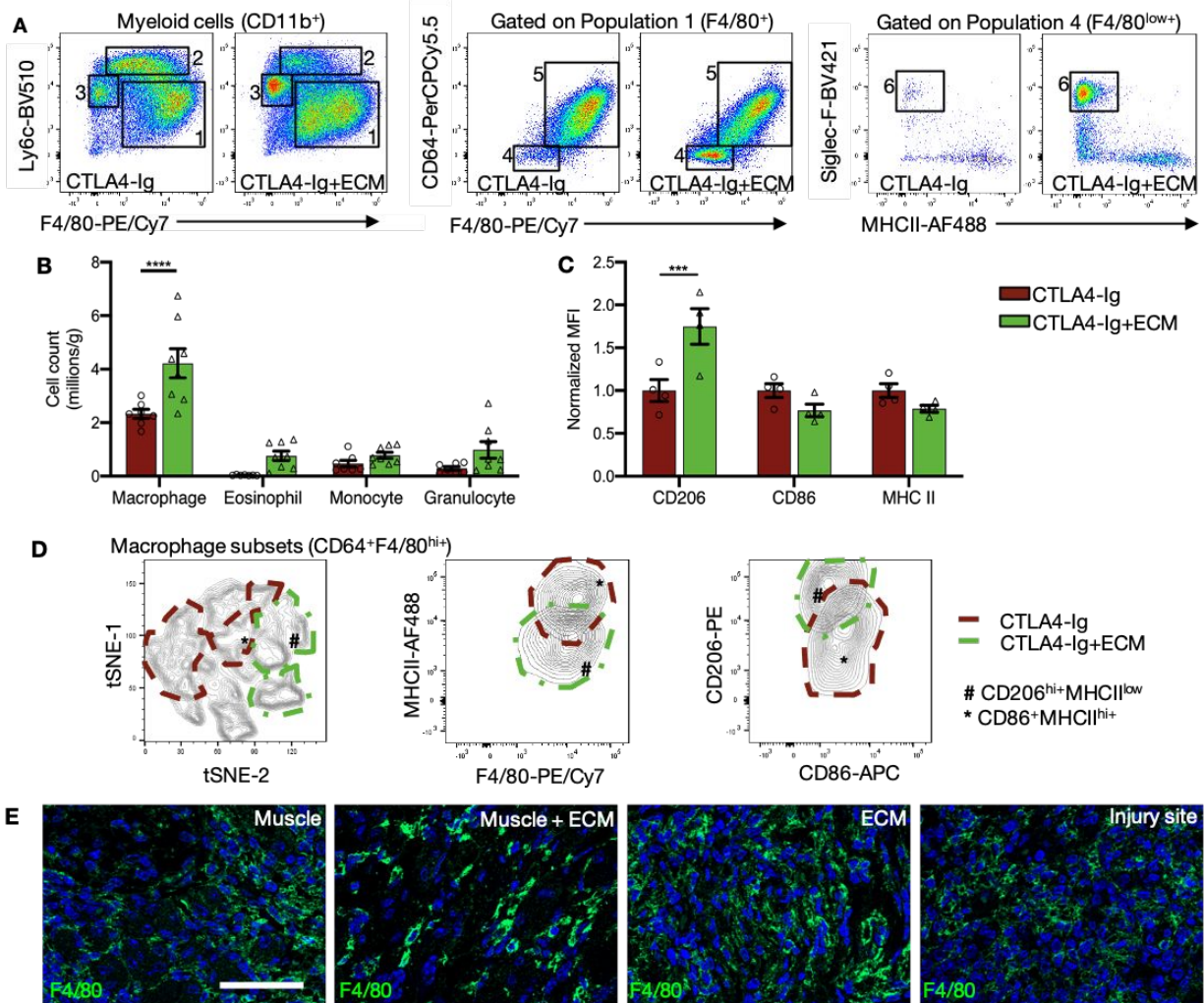


Figure 2: ECM reshapes myeloid infiltration (A) Representative flow cytometry shows CD11b⁺ myeloid cells populations modulated by ECM in murine hindlimb allografts treated with CTLA4-Ig at POD 14. Gates are Ly6c^{hi+} Monocytes (2), Ly6c^{mid+} Granulocytes (3), CD64⁺F4/80^{hi+} macrophages (5), SiglecF⁺F4/80^{low} Eosinophils (6). (B) Myeloid cell recruitment for CTLA4-Ig (red) or CTLA4-Ig with ECM (green) treatment groups show macrophages are significantly increased. Values are presented as mean \pm standard error mean (SEM), two-way ANOVA with Sidak post hoc analysis, $p < 0.05$. (C) Relative expression of macrophage polarization markers CD206 (M2-like), significant increase with ECM treatment, CD86 (M1-like) and MHCII did not. (D) Multidimensional flowcytometry data for a computational aggregate of CD64⁺F4/80^{hi+} macrophages in tSNE projection shows subsets exclusive to CTLA4-Ig+ECM (green) and CTLA4-Ig (red) conditions with distinctive activation marker profiles (# CD206^{hi+}MHCII^{low}, * CD86⁺MHCII^{hi+}). (E) Representative F4/80 infiltrates (green) with nuclei (DAPI, blue) across ECM and surrounding tissue from a CTLA4-Ig + ECM treated VCA, scale bar = 50 μ m.

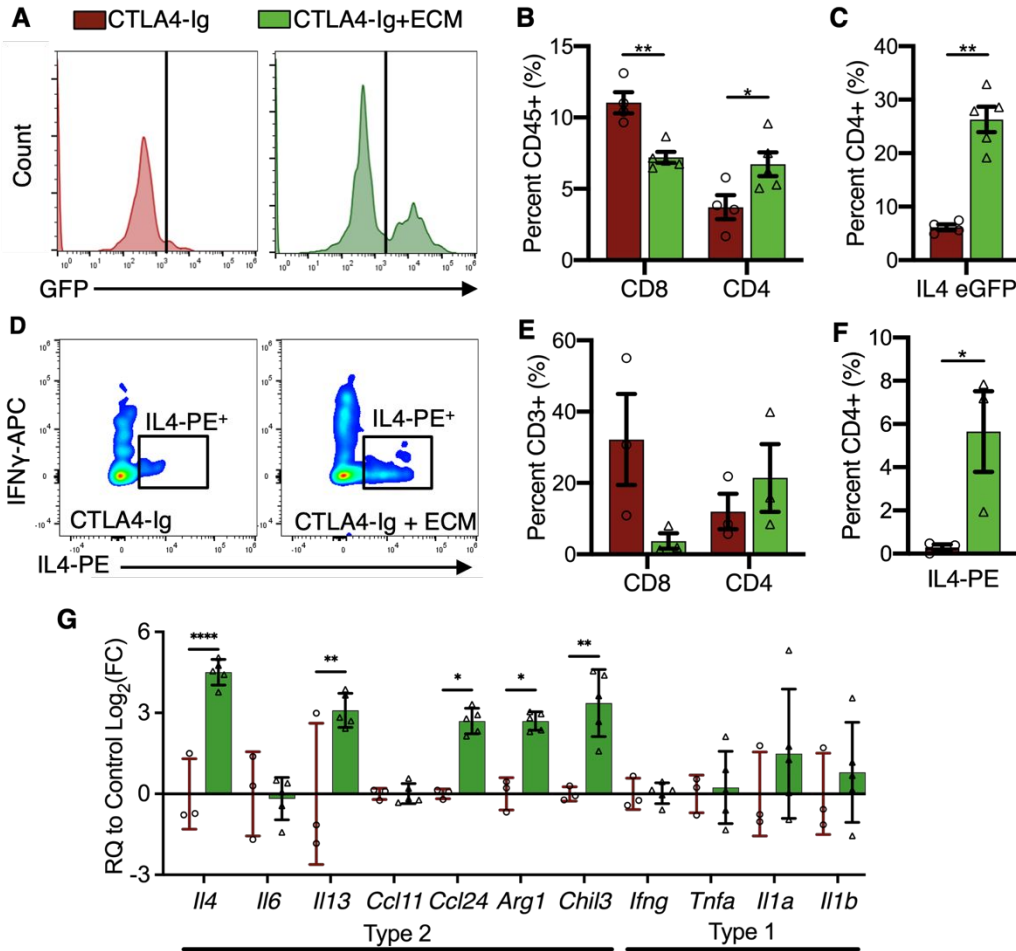


Figure 3: ECM treatment increases pro-regenerative Type 2 in CD4+ T helper cells. (A-C) ECM and CTLA4-Ig costimulatory blockade produce a local CD4+IL-4+ subset in allograft of 4get-GFP reporter mice (D-F) Intracellular cytokine staining confirms increased IL-4+ in circulating CD4+ fraction ECM treated mice. Values are presented as mean \pm SEM. (G) Gene expression of whole tissue isolate. Relative gene expression is represented by Log₂(FC) as mean \pm SD. Two-way ANOVA with Sidak post hoc analysis in B, E, G or t-test in C, F. *p < 0.05, ** p < 0.01, ***p < 0.001, and ****p < 0.0001.

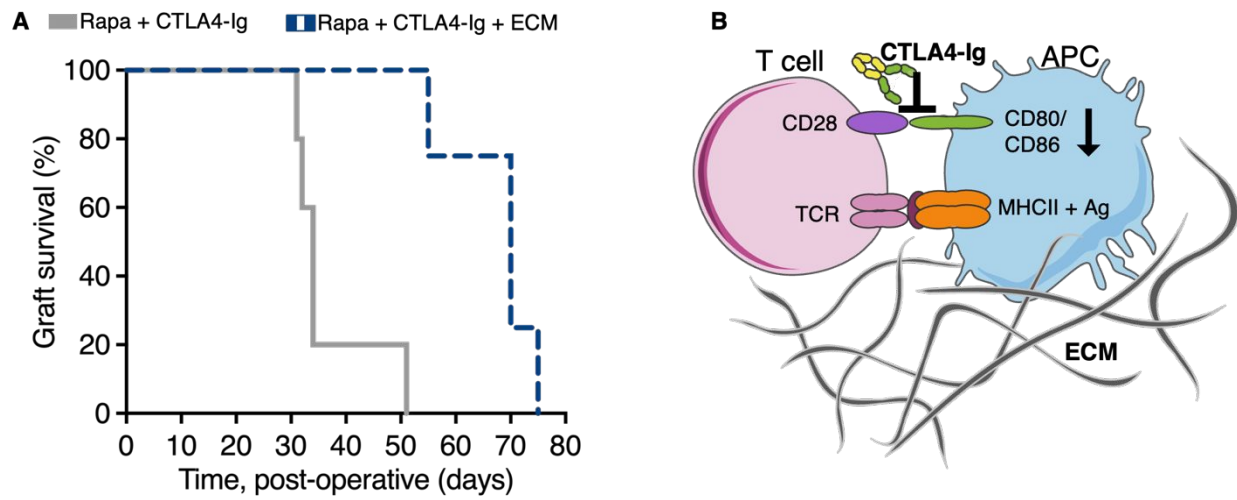


Figure 4: ECM combination therapy extends transplant survival (A) VCA survival was further extended by short-course Rapamycin treatment in combination with CTLA4-Ig and ECM treatment (MST = 70, $P = 0.0051$; Mantel-Cox) (B) Biologic scaffolds and CTLA4-Ig costimulatory blockade work synergistically.

1. K. Edtinger, X. Yang, H. Uehara and S. G. Tullius, *Burns Trauma*, 2014, **2**, 53-60.
2. A. L. Caplan, B. Parent, J. Kahn, W. Dean, L. L. Kimberly, W. P. A. Lee and E. D. Rodriguez, *Transplantation*, 2019, **103**, 1240-1246.
3. C. L. Kaufman, R. Ouseph, M. R. Marvin, Y. Manon-Matos, B. Blair and J. E. Kutz, *Curr Opin Organ Transplant*, 2013, **18**, 652-658.
4. J. T. Shores, G. Brandacher and W. P. A. Lee, *Plast Reconstr Surg*, 2015, **135**, 351e-360e.
5. G. Opelz, B. Dohler and S. Collaborative Transplant, *Transplantation*, 2009, **87**, 795-802.
6. P. Petruzzo, A. Gazarian, J. Kanitakis, H. Parmentier, V. Guigal, M. Guillot, C. Vial, J. M. Dubernard, E. Morelon and L. Badet, *Ann Surg*, 2015, **261**, 213-220.
7. F. Messner, J. Grahammer, T. Hautz, G. Brandacher and S. Schneeberger, *Curr Opin Organ Transplant*, 2016, **21**, 503-509.
8. S. G. Tullius, A. Reutzel-Selke, F. Egermann, M. Nieminen-Kelha, S. Jonas, W. O. Bechstein, H. D. Volk and P. Neuhaus, *J Am Soc Nephrol*, 2000, **11**, 1317-1324.
9. S. P. Pradka, Y. S. Ong, Y. Zhang, S. J. Davis, A. Baccarani, C. Messmer, T. A. Fields, D. Erdmann, B. Klitzman and L. S. Levin, *Transplant Proc*, 2009, **41**, 531-536.
10. F. Shimizu, O. Okamoto, K. Katagiri, S. Fujiwara and F. C. Wei, *Microsurgery*, 2010, **30**, 132-137.
11. C. A. Su, S. Iida, T. Abe and R. L. Fairchild, *Am J Transplant*, 2014, **14**, 568-579.
12. N. Chun, R. L. Fairchild, Y. Li, J. Liu, M. Zhang, W. M. Baldwin, 3rd and P. S. Heeger, *Am J Transplant*, 2017, **17**, 2810-2819.
13. A. E. Morelli and A. W. Thomson, *Nat Rev Immunol*, 2007, **7**, 610-621.
14. B. C. Oh, G. J. Furtmuller, M. L. Fryer, Y. Guo, F. Messner, J. Krapf, S. Schneeberger, D. S. Cooney, W. P. A. Lee, G. Raimondi and G. Brandacher, *JCI Insight*, 2020, **5**.
15. N. Pilat, C. Klaus, C. Schwarz, K. Hock, R. Oberhuber, E. Schwaiger, M. Gattringer, H. Ramsey, U. Baranyi, B. Zelger, G. Brandacher, F. Wrba and T. Wekerle, *Am J Transplant*, 2015, **15**, 1568-1579.
16. Y. Li, X. X. Zheng, X. C. Li, M. S. Zand and T. B. Strom, *Transplantation*, 1998, **66**, 1387-1388.
17. C. R. Gilson, Z. Milas, S. Gangappa, D. Hollenbaugh, T. C. Pearson, M. L. Ford and C. P. Larsen, *J Immunol*, 2009, **183**, 1625-1635.
18. C. P. Larsen, S. J. Knechtle, A. Adams, T. Pearson and A. D. Kirk, *Am J Transplant*, 2006, **6**, 876-883.
19. F. Vincenti, C. Larsen, A. Durrbach, T. Wekerle, B. Nashan, G. Blanche, P. Lang, J. Grinyo, P. F. Halloran, K. Solez, D. Hagerty, E. Levy, W. Zhou, K. Natarajan, B. Charpentier and G. Belatacept Study, *N Engl J Med*, 2005, **353**, 770-781.
20. S. F. Badylak, D. O. Freytes and T. W. Gilbert, *Acta Biomater*, 2009, **5**, 1-13.
21. A. A. Reznichenko, *Different Biologic Grafts for Diaphragmatic Crura Reinforcement During Laparoscopic Repair of Large Hiatal Hernia: A Six-Year Single Surgeon Experience*, 2016.
22. T. W. Gilbert, T. L. Sellaro and S. F. Badylak, *Biomaterials*, 2006, **27**, 3675-3683.
23. S. E. Dreifuss, R. Wollstein, S. F. Badylak and P. J. Rubin, *Plastic and Aesthetic Research*, 2015, **2**, 282-283.
24. I. L. Valerio, P. Campbell, J. Sabino, C. L. Dearth and M. Fleming, *Regen Med*, 2015, **10**, 611-622.

25. C. Afaneh, J. Abelson, M. Schattner, Y. Y. Janjigian, D. Ilson, S. S. Yoon and V. E. Strong, *Ann Surg Oncol*, 2015, **22**, 1252-1257.
26. B. M. Sicari, J. L. Dziki, B. F. Siu, C. J. Medberry, C. L. Dearth and S. F. Badylak, *Biomaterials*, 2014, **35**, 8605-8612.
27. J. L. Dziki, B. M. Sicari, M. T. Wolf, M. C. Cramer and S. F. Badylak, *Tissue Eng Part A*, 2016, **22**, 1129-1139.
28. J. L. Dziki, D. S. Wang, C. Pineda, B. M. Sicari, T. Rausch and S. F. Badylak, *J Biomed Mater Res A*, 2017, **105**, 138-147.
29. H. Kimmel, M. Rahn and T. W. Gilbert, *J Am Col Certif Wound Spec*, 2010, **2**, 55-59.
30. J. Zografakis, G. Johnston, J. Haas, L. Berbiglia, T. Bedford, J. Spear, A. Dan and M. Pozsgay, *JSLs*, 2018, **22**.
31. B. N. Brown, R. Londono, S. Tottey, L. Zhang, K. A. Kukla, M. T. Wolf, K. A. Daly, J. E. Reing and S. F. Badylak, *Acta Biomater*, 2012, **8**, 978-987.
32. K. Sadtler, S. D. Sommerfeld, M. T. Wolf, X. Wang, S. Majumdar, L. Chung, D. S. Kelkar, A. Pandey and J. H. Elisseeff, *Semin Immunol*, 2017, **29**, 14-23.
33. M. T. Wolf, S. Ganguly, T. L. Wang, C. W. Anderson, K. Sadtler, R. Narain, C. Cherry, A. J. Parrillo, B. V. Park, G. Wang, F. Pan, S. Sukumar, D. M. Pardoll and J. H. Elisseeff, *Sci Transl Med*, 2019, **11**.
34. K. Sadtler, K. Estrellas, B. W. Allen, M. T. Wolf, H. Fan, A. J. Tam, C. H. Patel, B. S. Lubber, H. Wang, K. R. Wagner, J. D. Powell, F. Housseau, D. M. Pardoll and J. H. Elisseeff, *Science*, 2016, **352**, 366-370.
35. S. F. Badylak, J. E. Valentin, A. K. Ravindra, G. P. McCabe and A. M. Stewart-Akers, *Tissue Eng Part A*, 2008, **14**, 1835-1842.
36. B. M. Sicari, J. P. Rubin, C. L. Dearth, M. T. Wolf, F. Ambrosio, M. Boninger, N. J. Turner, D. J. Weber, T. W. Simpson, A. Wyse, E. H. Brown, J. L. Dziki, L. E. Fisher, S. Brown and S. F. Badylak, *Sci Transl Med*, 2014, **6**, 234ra258.
37. K. Sadtler, M. T. Wolf, S. Ganguly, C. A. Moad, L. Chung, S. Majumdar, F. Housseau, D. M. Pardoll and J. H. Elisseeff, *Biomaterials*, 2019, **192**, 405-415.
38. L. C. Rankin and D. Artis, *Cell*, 2018, **173**, 554-567.
39. R. L. Gieseck, 3rd, M. S. Wilson and T. A. Wynn, *Nat Rev Immunol*, 2018, **18**, 62-76.
40. J. A. Knipper, S. Willenborg, J. Brinckmann, W. Bloch, T. Maass, R. Wagener, T. Krieg, T. Sutherland, A. Munitz, M. E. Rothenberg, A. Niehoff, R. Richardson, M. Hammerschmidt, J. E. Allen and S. A. Eming, *Immunity*, 2015, **43**, 803-816.
41. J. E. Heredia, L. Mukundan, F. M. Chen, A. A. Mueller, R. C. Deo, R. M. Locksley, T. A. Rando and A. Chawla, *Cell*, 2013, **153**, 376-388.
42. L. Gong, J. Li, J. Zhang, Z. Pan, Y. Liu, F. Zhou, Y. Hong, Y. Hu, Y. Gu, H. Ouyang, X. Zou and S. Zhang, *Acta Biomater*, 2020, **117**, 246-260.
43. K. L. Spiller, S. Nassiri, C. E. Witherel, R. R. Anfang, J. Ng, K. R. Nakazawa, T. Yu and G. Vunjak-Novakovic, *Biomaterials*, 2015, **37**, 194-207.
44. G. J. Furtmuller, B. Oh, J. Grahammer, C. H. Lin, R. Sucher, M. L. Fryer, G. Raimondi, W. P. Lee and G. Brandacher, *J Vis Exp*, 2016, DOI: 10.3791/53483, 53483.
45. Y. Li, X. C. Li, X. X. Zheng, A. D. Wells, L. A. Turka and T. B. Strom, *Nat Med*, 1999, **5**, 1298-1302.
46. K. Shimizu, U. Schonbeck, F. Mach, P. Libby and R. N. Mitchell, *J Immunol*, 2000, **165**, 3506-3518.

47. S. M. Ensminger, B. M. Spriewald, O. Witzke, K. Morrison, A. van Maurik, P. J. Morris, M. L. Rose and K. J. Wood, *Transplantation*, 2000, **70**, 955-963.
48. S. M. Ensminger, O. Witzke, B. M. Spriewald, K. Morrison, P. J. Morris, M. L. Rose and K. J. Wood, *Transplantation*, 2000, **69**, 2609-2612.
49. T. Kawai, A. B. Cosimi, T. R. Spitzer, N. Tolckoff-Rubin, M. Suthanthiran, S. L. Saidman, J. Shaffer, F. I. Preffer, R. Ding, V. Sharma, J. A. Fishman, B. Dey, D. S. Ko, M. Hertl, N. B. Goes, W. Wong, W. W. Williams, Jr., R. B. Colvin, M. Sykes and D. H. Sachs, *N Engl J Med*, 2008, **358**, 353-361.
50. J. D. Scandling, S. Busque, S. Dejbakhsh-Jones, C. Benike, M. T. Millan, J. A. Shizuru, R. T. Hoppe, R. Lowsky, E. G. Engleman and S. Strober, *N Engl J Med*, 2008, **358**, 362-368.
51. S. I. Alexander, N. Smith, M. Hu, D. Verran, A. Shun, S. Dorney, A. Smith, B. Webster, P. J. Shaw, A. Lammi and M. O. Stormon, *N Engl J Med*, 2008, **358**, 369-374.
52. D. A. Leonard, C. L. Cetrulo, Jr., D. A. McGrouther and D. H. Sachs, *Transplantation*, 2013, **95**, 403-409.
53. J. T. Shores, V. Malek, W. P. A. Lee and G. Brandacher, *J Mater Sci Mater Med*, 2017, **28**, 72.
54. A. N. Peña, J. A. Garcia and J. H. Elisseeff, *Current Opinion in Biomedical Engineering*, 2021, **20**, 100321.
55. X. Wang, L. Chung, J. Hooks, D. R. Maestas, Jr., A. Lebid, J. I. Andorko, L. Huleihel, A. F. Chin, M. Wolf, N. T. Remlinger, M. A. Stepp, F. Housseau and J. H. Elisseeff, *Sci Adv*, 2021, **7**.
56. U. Sarig, H. Sarig, E. de-Berardinis, S. Y. Chaw, E. B. V. Nguyen, V. S. Ramanujam, V. D. Thang, M. Al-Haddawi, S. Liao, D. Seliktar, T. Kofidis, F. Y. C. Boey, S. S. Venkatraman and M. Machluf, *Acta Biomater*, 2016, **44**, 209-220.
57. M. T. Wolf, C. L. Dearth, C. A. Ranallo, S. T. LoPresti, L. E. Carey, K. A. Daly, B. N. Brown and S. F. Badylak, *Biomaterials*, 2014, **35**, 6838-6849.
58. B. M. Sicari, V. Agrawal, B. F. Siu, C. J. Medberry, C. L. Dearth, N. J. Turner and S. F. Badylak, *Tissue Eng Part A*, 2012, **18**, 1941-1948.
59. S. D. Sommerfeld, C. Cherry, R. M. Schwab, L. Chung, D. R. Maestas, Jr., P. Laffont, J. E. Stein, A. Tam, S. Ganguly, F. Housseau, J. M. Taube, D. M. Pardoll, P. Cahan and J. H. Elisseeff, *Sci Immunol*, 2019, **4**.
60. L. Huleihel, G. S. Hussey, J. D. Naranjo, L. Zhang, J. L. Dziki, N. J. Turner, D. B. Stolz and S. F. Badylak, *Sci Adv*, 2016, **2**, e1600502.
61. R. Sridharan, B. Cavanagh, A. R. Cameron, D. J. Kelly and F. J. O'Brien, *Acta Biomater*, 2019, **89**, 47-59.
62. F. S. Majedi, M. M. Hasani-Sadrabadi, T. J. Thauland, S. Li, L. S. Bouchard and M. J. Butte, *Biomaterials*, 2020, **252**, 120058.
63. T. Wekerle and M. Sykes, *Annu Rev Med*, 2001, **52**, 353-370.
64. C. H. Lin, Y. L. Wang, M. R. Anggelia, W. Y. Chuang, H. Y. Cheng, Q. Mao, J. A. Zelken, C. H. Lin, X. X. Zheng, W. P. Lee and G. Brandacher, *Am J Transplant*, 2016, **16**, 2030-2041.
65. A. W. Thomson, H. R. Turnquist and G. Raimondi, *Nat Rev Immunol*, 2009, **9**, 324-337.
66. R. Ferguson, J. Grinyo, F. Vincenti, D. B. Kaufman, E. S. Woodle, B. A. Marder, F. Citterio, W. H. Marks, M. Agarwal, D. Wu, Y. Dong and P. Garg, *Am J Transplant*, 2011, **11**, 66-76.

67. L. C. Cendales, J. Kanitakis, S. Schneeberger, C. Burns, P. Ruiz, L. Landin, M. Rimmelink, C. W. Hewitt, T. Landgren, B. Lyons, C. B. Drachenberg, K. Solez, A. D. Kirk, D. E. Kleiner and L. Racusen, *Am J Transplant*, 2008, **8**, 1396-1400.
68. K. J. Livak and T. D. Schmittgen, *Methods*, 2001, **25**, 402-408.